Mathematical Biosciences and Engineering

http://www.aimspress.com/journal/mbe

MBE, 20(5): 8561–8582.
DOI: 10.3934/mbe.2023376
Received: 31 October 2022
Revised: 30 December 2022
Accepted: 21 February 2023
Published: 03 March 2023

Research article

Data-driven control of hydraulic servo actuator: An event-triggered adaptive dynamic programming approach

Vladimir Djordjevic[1], Hongfeng Tao[2], Xiaona Song[3], Shuping He[4], Weinan Gao[5] and Vladimir Stojanovic[1,*]

[1] Faculty of Mechanical and Civil Engineering, University of Kragujevac, 36000 Kraljevo, Serbia
[2] Key Laboratory of Advanced Process Control for Light Industry of Ministry of Education, Jiangnan University, Wuxi 214122, China
[3] School of Information Engineering, Henan University of Science and Technology, Luoyang 471023, China
[4] Key Laboratory of Intelligent Computing and Signal Processing (Ministry of Education) School of Electrical Engineering and Automation, Anhui University, Hefei 230601, China
[5] State Key Laboratory of Synthetical Automation for Process Industries, Northeastern University, Shenyang 110819, China

* **Correspondence:** Email: vladostojanovic@mts.rs.

Abstract: Hydraulic servo actuators (HSAs) are often used in the industry in tasks that request great power, high accuracy and dynamic motion. It is well known that an HSA is a highly complex nonlinear system, and that the system parameters cannot be accurately determined due to various uncertainties, an inability to measure some parameters and disturbances. This paper considers an event-triggered learning control problem of the HSA with unknown dynamics based on adaptive dynamic programming (ADP) via output feedback. Due to increasing practical application of the control algorithm, a linear discrete model of HSA is considered and an online learning data driven controller is used, which is based on measured input and output data instead of unmeasurable states and unknown system parameters. Hence, the ADP-based data driven controller in this paper requires neither the knowledge of the HSA dynamics nor exosystem dynamics. Then, an event-based feedback strategy is introduced to the closed-loop system to save the communication resources and reduce the number of control updates. The convergence of the ADP-based control algorithm is also theoretically shown. Simulation results verify the feasibility and effectiveness of the proposed approach in solving the optimal control problem of HSAs.

Keywords: data-driven control; adaptive dynamic programming; event-triggered control; hydraulic servo actuator

1. Introduction

Important properties of the HSA, such as fast and accurate responses, a high force/mass ratio and relatively good stiffness, have attracted great interest in the HSA and its applications. In the last two decades, high-performance controller design of the HSA has attracted increasing attention due to the expanded performance requirements of technical systems in the industry [1–4].

A large number of machines driven by HSAs often work with high payloads in harsh and mostly external environments. As a result of variables of their environment, such as temperature, dust, humidity, wear, variable loads and disturbances, the HSA is usually subject to large uncertainties during operation. Hence, high-precision control of the HSA has always challenged researchers due to its unmodeled dynamics, large nonlinearities, parametric uncertainties, unmeasurable states in practice, etc. It is well known that it is impossible to determine most of the physical parameters of HSA components. While some HSA parameters are available only with certain accuracy, the other parameters are completely unknown. Dominant nonlinear sources existing in HSAs are impossibility of accurate determining parameters, which are very difficult to handle with high accuracy. These unknown parameters are caused by protection of proprietary data of individual manufacturers or indirect measuring and calculating, pressure losses, transient and turbulent flow conditions, friction, leakage characteristics, and generation discontinuous control signals to HSAs due to effects of saturation and changing the direction of servo valve. Furthermore, variable working conditions during operation, such as oil temperature, the bulk modulus, fluctuating supply pressure and pipe volume will lead to parameter changes, which worsen the existing control performances. These facts make it difficult to realize high-quality control of the HSA, which cannot be achieved without knowing the accurate HSA model [5–8].

Further, direct measurement of the whole HSA state vector is not feasible for practical implementation and in addition would require very expensive measurement equipment. It is more convenient to use control algorithms which apply methods based on state reconstruction rather than to perform direct measurements of the states [9].

In modern control theory, optimal control of the HSA plays a vital role in the controller design. Namely, the main challenge is to design optimal control algorithms that will affect the minimum energy consumption [10, 11]. The optimal control design is an offline control technique that usually depends on perfect knowledge of the HSA model, which is not possible to obtain in most practical situations. Even if an approximated model of the HSA can be developed, the dynamic uncertainty, produced by the mismatch between the approximated model and the true HSA model, will degrade the control performance of the traditionally designed optimal controller [9, 12]. Therefore, further research on the design of optimal controllers of HSAs is very important and our primary aim for this study.

The practical applicability of control algorithms is enhanced by the fact that nonlinear systems can be very precisely represented by linear models with online estimated dynamics [13, 14]. Many modern engineering applications such as intelligent vehicles [15, 16], modernized microgrids [17], microphone sensing [18], strain prediction for fatigue [19], maintaining the security of cyber–physical systems [20], robotic manipulation tasks [21], 2-degree-of-freedom helicopter [22] and requests for online controller design which rely on linear systems.

Adaptive dynamic programming (ADP) ensures an effective way to achieve high performance of the optimal controller which relies on adaptive control, optimal control and reinforcement learning [9, 23–26]. ADP represents a kind of data-based control technique which can guarantee the stability

of the feedback control system [9]. Recently, the field of ADP application has also been expanded to various research areas, including robotic systems, aerospace systems, guided missiles, spacecraft, etc. [27–29]. In circumstances of unknown system dynamics and unmeasurable states, of great interest is to use ADP techniques based on measured input/output data from linear systems, which are commonly called output feedback. A main benefit of the output feedback techniques is that knowledge of the HSA dynamics is not needed for their application. For an unknown HSA model, this indirect technique generates a sequence of suboptimal controllers which converge to the optimal control policy with an increasing number of iterations.

The implementation of ADP algorithms is usually based on periodic selection [30]. In order to save limited communication and computational resources, event-triggered strategies have recently started to be applied in control algorithms based on ADP [31–34]. Moreover, the number of updates of the control inputs in this way will be smaller compared to the periodic update of the controller, because it is updated only when necessary (e.g., when the performance of the system deteriorates). The implementation of event-triggered algorithms is based on aperiodic sampling. Several event-based controllers have been proposed in the literature, most of which are state-feedback controllers [35–39]. In contrast, this paper will consider the event-triggered ADP-based control problem of HSAs in the case where only output feedback is available.

This paper considers an online learning technique, where during operation, from measured input/output data, the controller learns to compensate unknown HSA dynamics, various disturbances and modeling errors, ensuring desired performances of the control system. The optimal control law is accomplished iteratively based on output feedback, state reconstruction and ADP. The unknown HSA model is first identified after which the algebraic Riccati equation (ARE) is iteratively solved. To ensure consistency of approximations and obtain unique solutions in each iteration step, some exploration noise must be added to control input to meet the requirements of the persistent excitation condition [40–42]. For exploration noise, some persistent excitation is usually applied such as white noise or pseudo random binary signals (PRBS). The selection of exploration noise is a non-trivial task for the most learning problems, as it can affect the accuracy of solutions, especially for large systems [43]. By applying the theory of experimental design, we will use the sum of sinusoidal signals as an exploration noise that will enable the output of the system to carry maximum information about the system, which will shorten the learning time, i.e., speed up the controller design process. Thus, the obtained input and output signals are used to reconstruct the state vector of the model, which is of great practical importance in relation to control techniques with direct state measurement that rely on a large number of sensors.

Due to implementation of the ADP-based control techniques, it is easier to realize data acquisition for the discrete-time HSA model in relation to its continuous-time model. ADP-based control methodology for discrete-time systems is proposed in [44].

We chose to use the measured input and output data to reconstruct the state vector of the discretized HSA model, after which ADP-based control can be implemented. The control law is learned iteratively and very efficiently provides solutions for optimal control of HSAs based only on measurements in real time. The main advantage of the proposed control methodology is avoiding the knowledge of system dynamics, which is very important under practical conditions.

By applying an event-based control strategy, the number of control input updates will be reduced relative to periodic update of the controller, because the controller is only updated when certain con-

ditions are met. In this way, energy, computing and communication resources will be significantly preserved.

The rest of the paper is organized as follows. The problem of modelling an HSA with unknown dynamics is presented in Section 2. Event-triggered control based on ADP is shown in Section 3. Simulation results show the validity and effectiveness of the event-triggered ADP-based controller for HSAs in the presence of completely model uncertainty in Section 4. Finally, Section 5 gives the concluding remarks.

2. Description of the HSA

The HSA under study is shown in Figure 1, and it consists of a servo valve and a hydraulic cylinder. The analysis of the properties of the HSA comes out from the dynamics of its components, which involves the piston motion dynamics, pressure dynamics at the cylinder and servo valve dynamics. Hence, the model of the HSA is derived from complex nonlinear equations that depend on many parameters which cannot be accurately obtained [7, 8].

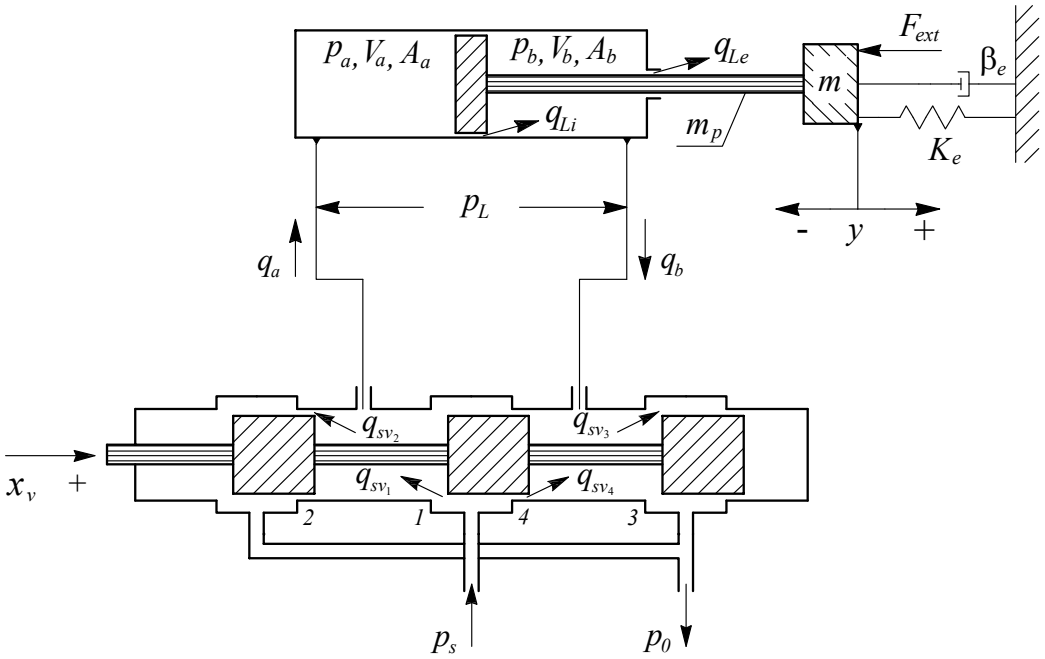

Figure 1. The HSA configuration.

See Table 1 for the description of the HSA parameters. Using the notation in Figure 1, and defining the area ratio of the piston $\alpha = A_b/A_a$ as well as $V_a = V_{a0} + yA_a$, $V_b = V_b0 + (L - y)\alpha A_a$ and $q_{Li} = c_{Li}(p_a - p_b)$, where c_{Li} is the internal leakage flow coefficient; $c_{vi} > 0$ denote discharge coefficients, the sign function $\mathrm{sg}(x) = \begin{cases} x & x \geq 0 \\ 0 & x < 0 \end{cases}$ and assuming an external leakage negligible, the considered model

can be described by the following equations:

$$m_t\ddot{y} = A_a p_a - A_b p_b - F_f(\dot{y}) - K_e y - -F_{ext}, \tag{2.1}$$

$$\dot{p}_a = \frac{\beta_e}{V_a(y)}\left(q_a - A_a\dot{y} - q_{Li} - q_{Lea}\right), \tag{2.2}$$

$$\dot{p}_b = \frac{\beta_e}{V_b(y)}\left(q_b + \alpha A_a\dot{y} + q_{Li} - q_{Leb}\right), \tag{2.3}$$

$$q_a = q_{sv1} - q_{sv2} = c_{v_1}\mathrm{sg}(x_v)\mathrm{sign}(p_s - p_a)\sqrt{|p_s - p_a|} - c_{v_2}\mathrm{sg}(-x_v)\mathrm{sign}(p_a - p_0)\sqrt{|p_a - p_0|}, \tag{2.4}$$

$$q_b = q_{sv3} - q_{sv4} = c_{v_3}\mathrm{sg}(-x_v)\mathrm{sign}(p_s - p_b)\sqrt{|p_s - p_b|} - c_{v_4}\mathrm{sg}(x_v)\mathrm{sign}(p_b - p_0)\sqrt{|p_b - p_0|}. \tag{2.5}$$

Table 1. Parameters of the HSA.

Notations	Descriptions
x_v	The spool valve displacement
p_a, p_b	Forward and return pressure
q_a, q_b	Forward and return flows
y	Piston displacement
L	Piston stroke
K_e	Load spring gradient
p_S, p_0	Supply and tank pressure
m_t, m_p, m	total mass, piston mass, payload mass
F_f	Friction force
F_{ext}	Disturbance force
A_a,A_b	Effective areas of the head and rod piston side
V_a, V_b, V_{a0}, V_{b0}	Fluid volumes of the head and rod piston side and corresponding initial volumes
q_{Li}, q_{Le}	Internal and external leakage flow
β_e	Bulk modulus of the fluid

According to Eqs (2.1)–(2.5), and by defining the state and input variables as

$$x(t) = \begin{bmatrix} x_1(t) & x_2(t) & x_3(t) & x_4(t) \end{bmatrix}^T \triangleq \begin{bmatrix} y(t) & \dot{y}(t) & p_a(t) & p_b(t) \end{bmatrix}^T, \tag{2.6}$$

$$u(t) = x_v(t), \tag{2.7}$$

the governing nonlinear continuous-time dynamics of the HSA can be expressed in a state-space form as follows:

$$\begin{aligned} \dot{x}(t) &= f(x(t)) + g(x(t), u(t)) + h(t), \\ y(t) &= \eta(x(t)), \end{aligned} \tag{2.8}$$

where $f(x(t))$ and $g(x(t), u(t))$ are the state dynamics and the input function, respectively:

$$f(x(t)) = \begin{bmatrix} x_2 \\ \frac{1}{m_t}\left(A_a x_3 - \alpha A_a x_4 - F_f(x_2) - K_e x_1\right) \\ -\frac{\beta_e}{A_a x_1 + V_{a0}}\left(A_a x_2 + c_{Li}(x_3 - x_4)\right) \\ \frac{\beta_e}{\alpha A_a (L - x_1) + V_{b0}}\left(\alpha A_a x_2 + c_{Li}(x_3 - x_4)\right) \end{bmatrix},$$

$$g(x(t), u(t)) = \begin{bmatrix} 0 \\ 0 \\ \frac{\beta_e}{A_a x_1 + V_{a0}}\left(c_{v_1}\mathrm{sg}(u)\mathrm{sign}(p_s - x_3)\sqrt{|p_s - x_3|} - \right. \\ \qquad \left. - c_{v_4}\mathrm{sg}(-u)\mathrm{sign}(x_3 - p_0)\sqrt{|x_3 - p_0|}\right) \\ \frac{\beta_e}{\alpha A_a (L - x_1) + V_{b0}}\left(c_{v_3}\mathrm{sg}(-u)\mathrm{sign}(p_s - x_4)\sqrt{|p_s - x_4|} - \right. \\ \qquad \left. - c_{v_2}\mathrm{sg}(u)\mathrm{sign}(x_4 - p_0)\sqrt{|x_4 - p_0|}\right) \end{bmatrix},$$

where output function $\eta(x(t)) = x_1(t)$ and disturbance function $h(t) = \begin{bmatrix} h_1(t) & -F_{ext}/m_t + h_2(t) & h_3(t) & h_4(t) \end{bmatrix}$ include loads, unmodelled dynamics and parameter uncertainties.

One of the main nonlinearities of the cylinder model is the nonlinear friction force F_f, which consists of static friction, Coulomb friction and Stribeck effect of velocity. An extensive study related to acting friction forces upon the HSA can be found in [7]. Further, we consider the linearized model of the HSA, whose parameters are experimentally identified for different working points of the HSA (i.e., different positions and external load conditions) [8]. Now, the model equations are expressed in a more suitable way in terms of the load pressure:

$$p_L = p_a - \alpha p_b, \tag{2.9}$$

which leads to simplified dynamic equations. At last, using the new state vector $\begin{bmatrix} x_1(t) & x_2(t) & x_3(t) \end{bmatrix}^T \triangleq \begin{bmatrix} y(t) & \dot{y}(t) & p_L(t) \end{bmatrix}^T$ allows us to express the HSA in a more compact form. Taking an operating point $x_0 \triangleq \begin{bmatrix} y_0 & \dot{y}_0 & p_{L0} \end{bmatrix}^T$, and assuming dominance of the first order term from the Taylor series expansion, the linearized continuous-time description of the reduced order is stated as follows

$$\dot{x}(t) = Ax(t) + B(t)u(t), \tag{2.10}$$

$$y(t) = Cx(t), \tag{2.11}$$

where $A = \begin{bmatrix} 0 & 1 & 0 \\ 0 & -\frac{B_C}{m_t} & \frac{A_a}{m_t} \\ 0 & -K_d & K_p \end{bmatrix}$, $B = \begin{bmatrix} 0 & 0 & K_x \end{bmatrix}^T$ and $C = \begin{bmatrix} 1 & 0 & 0 \end{bmatrix}$. The sensibility constants can be found as follows:

$$K_d = A_a\left(\frac{\beta_e}{V_A} + \alpha^2\frac{\beta_e}{V_B}\right)^{-1},$$

$$K_p = \frac{\beta_e\left(K_{pA} - C_{Li}\left(1 + \alpha^2\right)\right)}{V_A\left(1 + \alpha^2\right)} - \frac{\alpha\beta_e\left(K_{pB}\alpha^2 + C_{Li}\left(1 + \alpha^2\right)\right)}{V_B\left(1 + \alpha^2\right)},$$

$$K_x = \frac{\beta_e}{V_A}K_{xA} - \alpha\frac{\beta_e}{V_B}K_{xB},$$

where the flow sensibility constants regarding the pressure at the cylinder chambers are stated as:

$$K_{pA} = \begin{cases} \frac{-c_v x_{v0}}{\sqrt{p_s - p_{A0}}} & \text{for } x_v > 0 \\ \frac{-c_v x_{v0}}{\sqrt{p_{A0} - p_0}} & \text{for } x_v < 0 \end{cases}, \tag{2.12}$$

$$K_{pB} = \begin{cases} \frac{-c_v x_{v0}}{\sqrt{p_{B0} - p_0}} & \text{for } x_v > 0 \\ \frac{-c_v x_{v0}}{\sqrt{p_s - p_{B0}}} & \text{for } x_v < 0 \end{cases}, \tag{2.13}$$

and the flow sensibility constants regarding the spool position are stated as

$$K_{xA} = \begin{cases} c_v \sqrt{p_s - p_{A0}} & \text{for } x_v > 0 \\ -c_v \sqrt{p_{A0} - p_0} & \text{for } x_v < 0 \end{cases}, \tag{2.14}$$

$$K_{xB} = \begin{cases} -c_v \sqrt{p_{B0} - p_0} & \text{for } x_v > 0 \\ c_v \sqrt{p_s - p_{B0}} & \text{for } x_v < 0 \end{cases}. \tag{2.15}$$

The previously mentioned valve sensibility constants are very significant in defining system stability and other dynamic characteristics [8]. Namely, the flow gain K_x has a direct impact on the stability of the HSA, because it directly affects the gain constant in the open loop of the HSA. Further, direct impact on the damping ratio of the HSA has the flow-pressure constant K_p. Hence, the pressure sensibility $K_{p_x} = K_x/K_p$ is quite high, which explains the ability of the HSA to transfer large friction loads with a small error.

3. Event-triggered ADP-based controller

Let us consider a linear continuous-time model of the HSA with unknown dynamics, as follows:

$$\dot{x}(t) = Ax(t) + Bu(t), \tag{3.1}$$

$$y(t) = Cx(t), \tag{3.2}$$

where $x(t) \in \mathbb{R}^n$, $u(t) \in \mathbb{R}^m$ and $y(t) \in \mathbb{R}^r$ are the system state vector, the control input vector, and the output vector, respectively. $A \in \mathbb{R}^{n\times n}$, $B \in \mathbb{R}^{n\times m}$ and $C \in \mathbb{R}^{r\times n}$ are unknown system matrices, assuming that (A, B) is controllable and (A, C) is observable.

For the HSA described by (3.1) and (3.2), the performance index is stated as

$$J(x_0) = \int_0^\infty \left[y^T(\tau) Q y(\tau) + u^T(\tau) R u(\tau) \right] d\tau, \tag{3.3}$$

where $x_0 \in \mathbb{R}^n$ is an initial state, $Q = Q^T \geq 0$ and $R = R^T > 0$, with $(A, Q^{1/2}C)$ being observable.

A control law is also called a policy. The design objective is to find a linear optimal control policy in the form of

$$u = -K^* x, \tag{3.4}$$

which minimizes the performance given by index (3.3). The optimal feedback gain matrix K^*can be determined as

$$K^* = R^{-1} B^T P^*, \tag{3.5}$$

where $P^* = (P^*)^T > 0$ is a unique symmetric positive definite solution of the well-known ARE

$$A^T P^* + P^* A + C^T Q C - P^* B R^{-1} B^T P^* = 0, \tag{3.6}$$

under conditions that the system matrices are accurately known, as well as conditions that the pair (A, B) is controllable and the pair $(A, Q^{1/2}C)$ is observable [12]. It should be noted that this optimal control design is mainly applicable to low order simple linear systems. In fact, for high-order large scale systems, it is usually difficult to directly solve P^* from (3.6), which is nonlinear in P.

Also, for practical implementation of the control system, it is easier to realize the data acquisition for discrete-time systems than for continuous-time systems. Consequently, we transform the continuous-time HSA into the following discrete-time HSA:

$$x_{k+1} = A_d x_k + B_d u_k, \tag{3.7}$$

$$y_k = C x_k, \tag{3.8}$$

where $A_d = e^{Ah}$ and $B_d = \int_0^h \left(e^{A\tau} d\tau\right) B$, where $h > 0$ is a specific sampling period, assuming $\omega_h = 2\pi/h$ is the nonpathological sampling frequency whose existence is well known [45]. In other words, the controllability and observability of the original continuous-time HSA system is kept after discretization. Namely, if the state, input and output vectors at the sampled instant kh are x_k, u_k and y_k, respectively, then (A_d, C) and $\left(A_d, Q^{1/2}C\right)$ are observable while (A_d, B_d) is controllable.

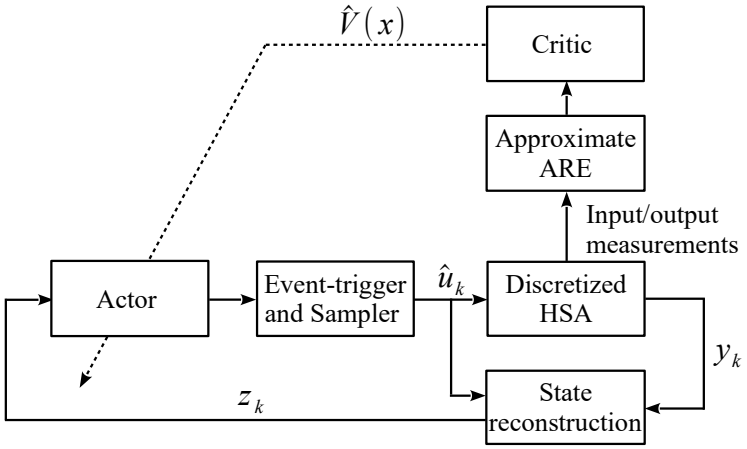

Figure 2. Event-triggered ADP-based control algorithm for the discretized HSA system.

As depicted in Figure 2, the ADP-based controller for the discretized HSA system consists of three parts: the state reconstruction, critic, and actor. The state reconstruction provides the relationship between the input/output data and the HSA states, which allows one to solve the optimal control problem

of an HSA with unknown dynamics. Based on the input/output data, the critic part of the controller is designed to evaluate the performance of the control policy. The controller learns online in order to maximize its performance. Finally, the actor applies the improved control policy. The updates of the control actions are governed by an event-triggering mechanism to reduce the amount of data transmission from the controller to the HSA system.

The event-triggered design is based on a periodic sampling with a nonpathological $h > 0$. We use $\hat{u}_k$ to represent the sampled value of u_k, that is

$$\hat{u}_k = u_{kj} \quad , k \in \left[k_j, k_{j+1}\right), \tag{3.9}$$

where $\left\{k_j\right\}_0^\infty$ is a monotonically increasing sequence of the sampling time instants, and the control input is only updated at the discrete-time instants: $k_0, k_1, k_2, \ldots$

For the convenience of discussions, define the sampling error of the input data as

$$\Delta_k = \hat{u}_k - u_k. \tag{3.10}$$

Hence, the discrete-time system described by (3.7) and (3.8) can be rewritten as

$$x_{k+1} = A_d x_k + \left(B_d u_k + \Delta_k\right), \tag{3.11}$$

$$y_k = C x_k. \tag{3.12}$$

Further, the performance index for the discretized system described by (3.7) and (3.8) is

$$J_d(x_0) = \sum_{j=0}^{\infty} y_j^T Q_d y_j + u_j^T R_d u_j, \tag{3.13}$$

where $Q_d = Qh$ and $R_d = Rh$. The optimal control low minimizing (3.13) is

$$u_k = -K_d^* x_k, \tag{3.14}$$

where the discrete optimal feedback gain matrix is $K_d^* = \left(R + B_d^T P_d^* B_d\right)^{-1} B_d^T P_d^* A_d$, where P_d^* is the unique symmetric positive definite solution to

$$A_d^T P_d^* A_d - P_d^* + C^T Q C - A_d^T P_d^* B_d K_d^* = 0. \tag{3.15}$$

Since (3.15) is nonlinear in P_d^* , it is difficult to directly solve P_d^* for high-order large-scale systems. Nevertheless, many efficient algorithms have been developed to numerically approximate the solution of (3.15). One of such algorithms was developed by Hewer [46], and it is introduced in the form of Lemma 3.1.

Lemma 3.1. *Let $K_0 \in \mathbb{R}^{m\times n}$ be any stability feedback gain matrix and P_j be the symmetric positive definite solution of the Lyapunov equation*

$$\left(A_d - B_d K_j\right)^T P_j \left(A_d - B_d K_j\right) + C^T Q_d C + K_j^T R_d K_j = 0, \tag{3.16}$$

where K_j, $j = 1, 2, \ldots$ can be updated as follows:

$$K_j = \left(R + B_d^T P_{j-1} B_d\right)^{-1} B_d^T P_{j-1} A_d. \tag{3.17}$$

Then, it holds that

1) $A_d - B_d K_j$ *is a stability matrix*

2) $P_d^* \leq P_{j+1} \leq P_j$

3) $\lim_{j\to\infty} K_j = K_d^*$, $\lim_{j\to\infty} P_j = P_d^*$.

By iteratively solving the Lyapunov equations given by (3.16), which is linear in P_j, and recursively updating the control policy K_j by (3.17), the solution to the nonlinear equation given by (3.15) is numerically approximated [46]. It has been concluded that the sequences $\left\{P_j\right\}_{j=0}^{\infty}$ and $\left\{K_j\right\}_{j=0}^{\infty}$, computed from this algorithm, converge to P_d^* and K_d^*, respectively. Moreover, for $j = 0, 1, \ldots$, $A_d - B_d K_j$ is a Schur matrix. It should be noted that the method by Hewers involves a model-based policy iteration (PI) algorithm, which cannot be directly applied to the problem studied in this paper since it is an offline algorithm which depends on the system parameters. To apply this algorithm online for the discretized HSA described by (3.7) and (3.8), we will develop the control algorithm based on ADP via output feedback, which does not depend on the knowledge of HSA matrices.

Motivated by [44,47], the discrete-time HSA described by (3.7) and (3.8) can be extended by using input/output sequences on the time horizon $[k-N, k-1]$ as follows:

$$\begin{aligned} x_k &= A_d^N x_{k-N} + V(N)\bar{u}_{k-1,k-N}, \\ \bar{y}_{k-1,k-N} &= U(N)x_{k-N} + T(N)\bar{u}_{k-1,k-N}, \end{aligned} \tag{3.18}$$

where

$$\begin{aligned} \bar{\Delta}_k &= \begin{bmatrix} \Delta_{k-1}^T & \Delta_{k-2}^T & \ldots & \Delta_{k-N}^T \end{bmatrix}^T, \\ \bar{u}_{k-1,k-N} &= \begin{bmatrix} \hat{u}_{k-1}^T & \hat{u}_{k-2}^T & \ldots & \hat{u}_{k-N}^T \end{bmatrix}^T, \\ \bar{y}_{k-1,k-N} &= \begin{bmatrix} y_{k-1}^T & y_{k-2}^T & \ldots & y_{k-N}^T \end{bmatrix}^T, \\ V(N) &= \begin{bmatrix} B_d & A_d B_d & \ldots & A_d^{N-1} B_d \end{bmatrix}], \\ U(N) &= \begin{bmatrix} (CA_d^{N-1})^T & (CA_d)^T & \ldots & C^T \end{bmatrix}^T, \\ T(N) &= \begin{bmatrix} 0 & CB_d & CA_dB_d & \cdots & CA_d^{N-2}B_d \\ 0 & 0 & CB_d & \cdots & CA_d^{N-3}B_d \\ \vdots & \vdots & \ddots & \ddots & \vdots \\ 0 & 0 & \cdots & 0 & CB_d \\ 0 & 0 & \cdots & 0 & 0 \end{bmatrix}, \end{aligned}$$

and the observability index is $N = \max(\rho_u, \rho_v)$ where ρ_u is the minimum integer which ensures that $U(\rho_u)$ has full column rank and ρ_v is the minimum integer which ensures that $V(\rho_v)$ has full row rank [44]. Therefore, there exists a left inverse of $U(N)$, stated as $U^+(N) = \left[U^T(N)U(N)\right]^{-1} U^T(N)$. With the state reconstruction in (3.18), the idea of an ADP-based controller with output feedback can be applied to solve the optimal control problem of HSAs with unknown dynamics. A uniqueness of state reconstruction is stated in the form of Lemma 3.2 as follows [48].

Lemma 3.2. *If the conditions of observability and controllability of the system described by (3.7) and (3.8) are fulfilled, then the states of the HSA are uniquely received in terms of measured inputs and outputs signals as follows:*

$$x_k = \Theta z_k, \tag{3.19}$$

where $\Theta = \begin{bmatrix} M_u & M_y \end{bmatrix}$ *has full row rank,* $M_u = V(N) - M_y T(N)$, $M_y = A_d^N U^+(N)$ *and* $z_k = \begin{bmatrix} \bar{u}_{k-1,k-N}^T & \bar{y}_{k-1,k-N}^T \end{bmatrix}^T \in \mathbb{R}^q$, *where* $q = N[\dim(u) + \dim(y)]$.

Now, based on (3.16) and (3.17), an online learning strategy using output feedback can be introduced in the form of $u_k^* = -\overline{K}_d z_k$, providing suboptimal property of the closed-loop system. The discrete-time model (3.11) can be stated as follows:

$$x_{k+1} = A_j x_k + B_d \left(K_j x_k + \hat{u}_k \right), \tag{3.20}$$

where $A_j = A_d - B_d K_j$. Setting $\bar{K}_j = K_j \Theta$ and $\bar{P}_j = \Theta^T P_j \Theta$, from (3.16) and (3.20), it can be obtained

$$\begin{aligned}
&z_{k+1}^T \bar{P}_j z_{k+1} - z_k^T \bar{P}_j z_k = \\
&\left(\bar{K}_j z_k + \hat{u}_k \right)^T \begin{bmatrix} B_d^T \bar{P}_j B_d & B_d^T \bar{P}_j A_d \end{bmatrix} \begin{bmatrix} -\bar{K}_j z_k + \hat{u}_k \\ 2 z_k \end{bmatrix} - \left(y_k^T Q y_k + z_k^T \bar{K}_j^T R \bar{K}_j z_k \right) = \\
&\left[\hat{u}_k^T \otimes \hat{u}_k^T - (z_k^T \otimes z_k^T)(\bar{K}_j^T \otimes \bar{K}_j^T) \right] \mathrm{vec}(\bar{H}_j^1) + \\
&2 \left[(z_k^T \otimes z_k^T)(I_q \otimes \bar{K}_j^T) + (z_k^T \otimes u_k^T) \right] \mathrm{vec}(\bar{H}_j^2) - \left(y_k^T Q y_k + z_k^T \bar{K}_j^T R \bar{K}_j z_k \right) \triangleq \\
&\phi^1 \mathrm{vec}(\bar{H}_j^1) + \phi^2 \mathrm{vec}(\bar{H}_j^2) - \left(y_k^T Q y_k + z_k^T \bar{K}_j^T R \bar{K}_j z_k \right),
\end{aligned} \tag{3.21}$$

where $\bar{H}_j^1 = B_d^T \bar{P}_j B_d$, $\bar{H}_j^2 = B_d^T \bar{P}_j A_d \Theta$, $\phi^1 = \hat{u}_k^T \otimes \hat{u}_k^T - (z_k^T \otimes z_k^T)(\bar{K}_j^T \otimes \bar{K}_j^T)$ and $\phi^2 = 2 \left[(z_k^T \otimes z_k^T)(I_q \otimes \bar{K}_j^T) + (z_k^T \otimes \hat{u}_k^T) \right]$.

The symbol $\otimes$ is used to denote a Kronecker product operator. The vector function $\mathrm{vec}(V) = \begin{bmatrix} v_1^T & v_2^T & \dots & v_m^T \end{bmatrix}^T$ is stated as an mn-vector formed by stacking the columns of $V \in \mathbb{R}^{n \times m}$ on top of one another, where $v_i \in \mathbb{R}^n$ denotes the columns of matrix V. For an arbitrary symmetric matrix $M \in \mathbb{R}^{n \times n}$, $\mathrm{vecs}(M) = [m_{11}, 2m_{12}, \dots, 2m_{1n}, m_{22}, 2m_{23}, \dots, 2m_{n-1,n}, m_{nn}]^T \in \mathbb{R}^{n(n+1)/2}$ and for an arbitrary column vector $v \in \mathbb{R}^n$, $\tilde{v} = \left[v_1^2, v_1 v_2, \dots, v_1 v_n, v_2^2, v_2 v_3, \dots, v_{n-1} v_n, v_n^2 \right]^T \in \mathbb{R}^{n(n+1)/2}$.

The convergence of the online learning control using output feedback is guaranteed under the rank condition stated in the form of Lemma 3.3 [47]. Lemma 3.3 is about the condition of persistent excitation in adaptive control theory [49, 50].

Lemma 3.3. *Let us suppose that for a sufficiently large* $s \in \mathbb{Z}_+$, *it holds that*

$$rank(\Gamma) = (\dim(u) + \dim(z))(\dim(u) + \dim(z) + 1)/2, \tag{3.22}$$

where

$$\Gamma = [\eta_{k0} \otimes \eta_{k0}, \eta_{k1} \otimes \eta_{k1}, \cdots, \eta_{ks} \otimes \eta_{ks}], \text{ where } k_0 < k_1 < \cdots < k_s \in \mathbb{Z}_+ \text{ and } \eta_{kj} = [\hat{u}_{kj}^T, z_{kj}^T]^T, j = \overline{0, s}; \tag{3.23}$$

then $\left(\bar{P}_j, \bar{H}_j^1, \bar{H}_j^2 \right)$ *can be uniquely solved based on* $\bar{K}_j$ *and measurable online data during the period* $k \in [k_0, k_s]$. *Further,* $\bar{K}_{j+1}$ *is obtained as follows:*

$$\bar{K}_{j+1} = \left(R + \bar{H}_j^1 \right)^{-1} \bar{H}_j^2. \tag{3.24}$$

Some exploration noise e_k, which satisfies the persistent excitation condition, must be added into the input signal during the online learning phase due to the satisfaction of the rank condition given by

(3.22), without affecting the convergence of the learning phase [43, 51, 52]. Note that (3.21) is called the policy evaluation, which is used to uniquely solve $\bar{P}_j$, and (3.24) is the policy improvement, which is used to update the control gain $\bar{K}_{j+1}$. Finally, we present the ADP-based online learning control algorithm in Figure 3.

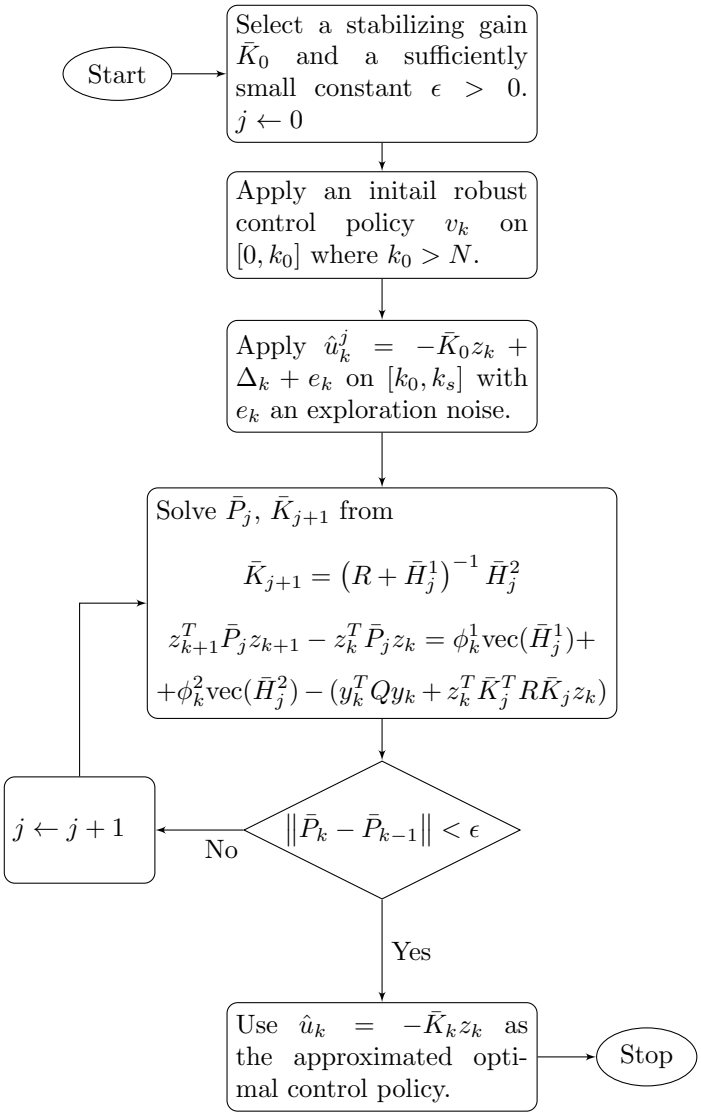

Figure 3. Flowchart of ADP-based controller design.

It should be noted that solving (3.21) instead of (3.16), completely eliminates the original request on the accurate knowledge of the HSA dynamics. Now, we only need to measure u_k and y_k. Namely, having in mind the expression for z_k, we can see that the control policy $\hat{u}_k = -\overline{K}_k^* z_k + \Delta_k$ contains only the previously measured input-output data. With the event-triggered control law $\hat{u}_k$, the system given by (3.20) is globally asymptotically stable (GAS) at the origin if

$$\|\Delta_k\|^2 \leq \frac{\alpha\gamma \|y_k\|^2 + \lambda_{\min}(R_d) \|\hat{u}_k\|^2}{\eta}, \tag{3.25}$$

where $\alpha \in (0, 1)$ and η is a positive constant satisfying $\eta \geq \lambda_{\max}\left(R_d + B_d^T \bar{P}_d B_d\right)$.

The convergence of the ADP-based control algorithm is presented in the form of Theorem 3.4. For Hurwitz feedback matrix $A - BK$, $K \in R^{m\times n}$ is called stabilizing feedback gain matrix for a linear system $\dot{x} = Ax + Bu$.

Theorem 3.4. *If the condition of Lemma 3.3 is fulfilled, with some initial stabilizing feedback gain matrix $\overline{K}_0$, then the sequences $\left\{\overline{P}_j\right\}_{j=0}^{\infty}$ and $\left\{\overline{K}_j\right\}_{j=0}^{\infty}$ received from this algorithm, converge to their optimal values $\overline{P}^*$ and $\overline{K}^*$, respectively [46, 47].*

Proof. If $P_j = P_j^T$ represents the solution of (3.16) , under the stability feedback gain matrix $\overline{K}_j$, then K_{j+1} is uniquely obtained from (3.17). It can be easily shown that $\overline{P}_j$ and $\overline{K}_{j+1}$ fulfill (3.21) and (3.24). Now, setting $\overline{P}$ and $\overline{K}$ as solutions of (3.21) and (3.24), Lemma 3.3 provides that $\overline{P}_j = \overline{P}$ and $\overline{K}_{j+1} = \overline{K}$ are uniquely stated. Furthermore, from Lemma 3.1, we have that $\lim\limits_{j\to\infty}\overline{K}_j = \overline{K}_d^*$ and $\lim\limits_{j\to\infty}\overline{P}_j = \overline{P}_d^*$. The proof of convergence is proved. □

The hybrid nature of the controller is shown in Figure 4. It is shown there that the feedback gain or policy is updated at discrete times by using (3.24) after the solution to (3.21) has been determined. On the other hand, the control input is a discrete time signal depending on the state $z(k)$ at each time k. From Figure 4, it can be seen that the control gains are updated at discrete times, but the control signal is piecewise continuous.

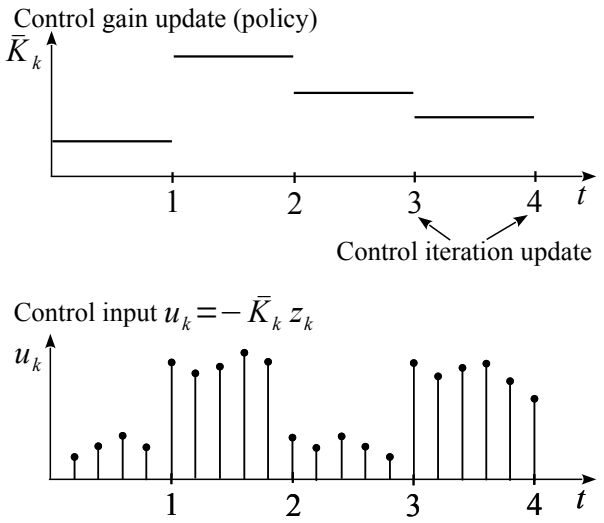

Figure 4. Hybrid nature of control signal.

4. Simulation results

In this section, we apply the proposed event-triggered ADP-based control design to the HSA. In the case of unknown dynamics and unmeasurable states of the HSA, it is meaningful to use the ADP-based method. Consequently, we conduct simulations on the HSA given by the linearized continuous-time description of (2.10) and (2.11) to show the effectiveness of the ADP-based control algorithm. A basic

condition for energy savings in many hydraulically driven industrial systems is a high-quality design of event-triggered ADP control for the HSA.

For this purpose, the HSA is discretized by applying the periodic sampling period $h = 0.1$ s and the zero-order holder. The approximated optimal feedback gain and performance index for the discretized model of the HSA are iteratively obtained.

The effectiveness of the ADP-based control algorithm will be considered for the HSA model described by (2.10) and (2.11) with the following parameters: the viscous friction $B_C = 200\,\mathrm{N\,s\,m^{-1}}$, the supply pressure $p_S = 45\,\mathrm{bar}$, the tank pressure $p_0 = 1.6\,\mathrm{bar}$, the bulk modulus of the fluid $\beta_e = 2 \times 10^8$ Pa, the total mass $m = 25\,\mathrm{kg}$, the initial chamber volumes $V_{a0} = V_{b0} = 8.2 \times 10^{-6}\,\mathrm{m^3}$, the load spring gradient $K_e = 10^{-1}$, the effective area of the head side of the piston $A_a = 4.91 \times 10^{-4}\,\mathrm{m^2}$, the effective area of the rod side of the piston $A_b = 2.43 \times 10^{-4}\,\mathrm{m^2}$, the internal leakage coefficient $c_{Li} = 5 \times 10^{-14}$, the piston stroke $L = 1\,\mathrm{m}$ and discharge coefficients of valve orifices $c_{vi} = 1.15$, $i = \overline{1,4}$.

For the purpose of demonstrating the event-triggered ADP method with the HSA, the weight matrices, Q and R, are chosen to be identity matrices, the observability index is $N = 3$, initial state vector is $x_0 = \begin{bmatrix} 5 & -5 & -10 \end{bmatrix}$ and the convergence threshold ε is selected as 10^{-1}.

It should be noted that our event-driven ADP control design does not require exact knowledge of the HSA matrices. But, only for numerical verification via simulation, it is assumed that the system matrices in (2.10) and (2.11) are known.

To verify the benefits of the ADP based online learning controller, Figure 5 depicts the errors between $\bar{P}_j$ and $\bar{P}_d^*$ and $\bar{K}_j$ and $\bar{K}_d^*$, which indicate the convergence of $\bar{P}_j$ and $\bar{K}_j$.

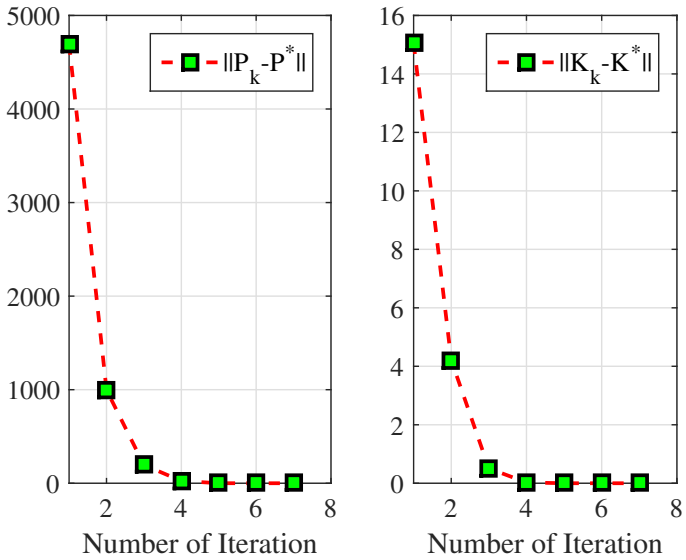

Figure 5. Convergence of $\bar{P}_j$ and $\bar{K}_j$ to their respective optimal values $\bar{P}^*$ and $\bar{K}^*$ during the learning process.

The evolution of the maximum cost for HSA is shown in Figure 6(a), where V_1 is the maximum cost by using the initial control policy, and V_7 is the maximum cost by using the control policy after seven iterations. It can be seen that the approximated cost function V_7 has been remarkably reduced relative

to the initial cost V_1. Figure 6(b) shows the 3D plot of the approximation error of the cost function. This error is close to zero which confirms that good approximation of the optimal cost function is achieved during the learning process.

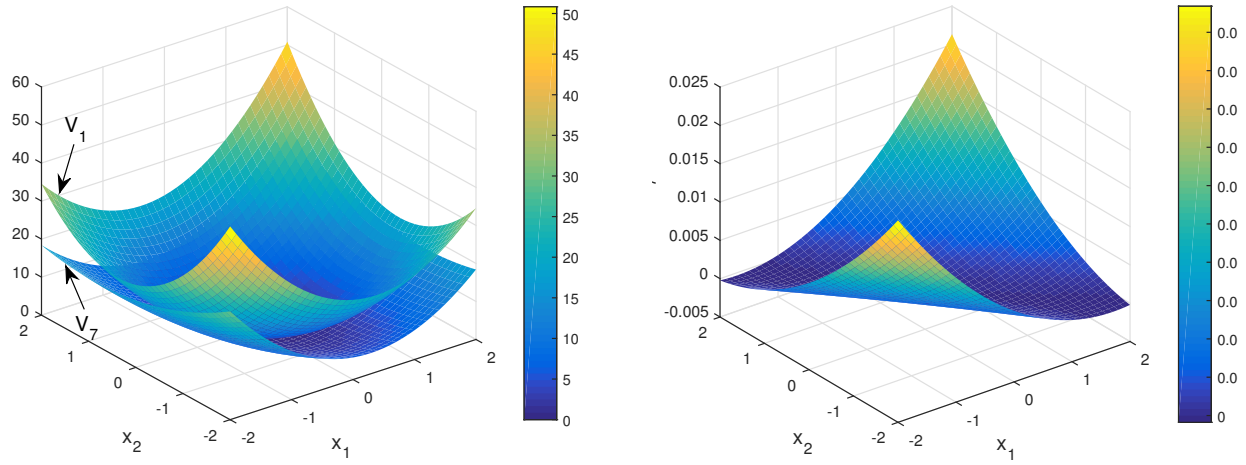

Figure 6. (a) Comparison of the cost functions during learning; (b) error between the optimal and approximated cost function signal.

The improved control policy and the initial control policy are compared in Figure 7(a). Further, Figure 7(b) shows the 3D plot of the difference between the approximated control obtained by using the online ADP-based control algorithm and the optimal control. This error is close to zero, which confirms that good approximation of the optimal input is also achieved during the learning process.

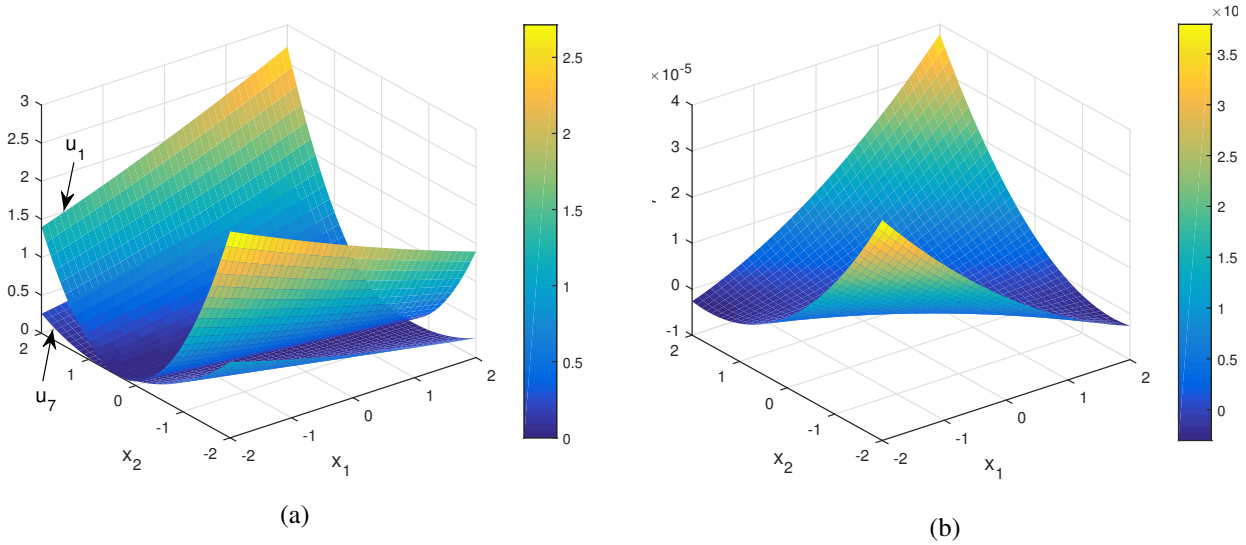

Figure 7. (a) Comparison of the control policies during the learning process; (b) error between the optimal and approximated input signal.

Figure 8 shows the control input and the states of the HSA system desribed by (2.10) and (2.11) by using the ADP-based controller with periodic sampling.

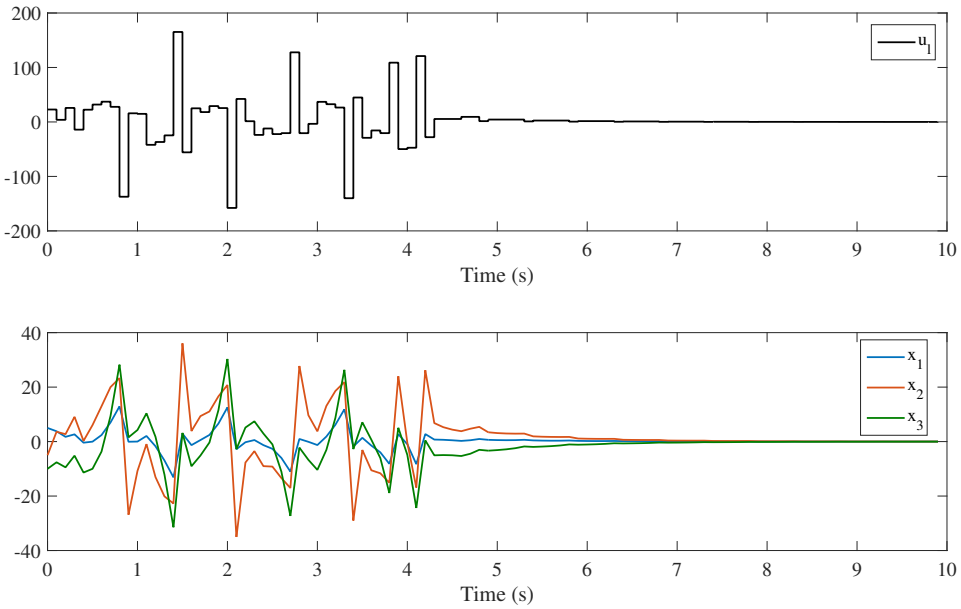

Figure 8. Control input and states of the HSA model by using the ADP-based controller.

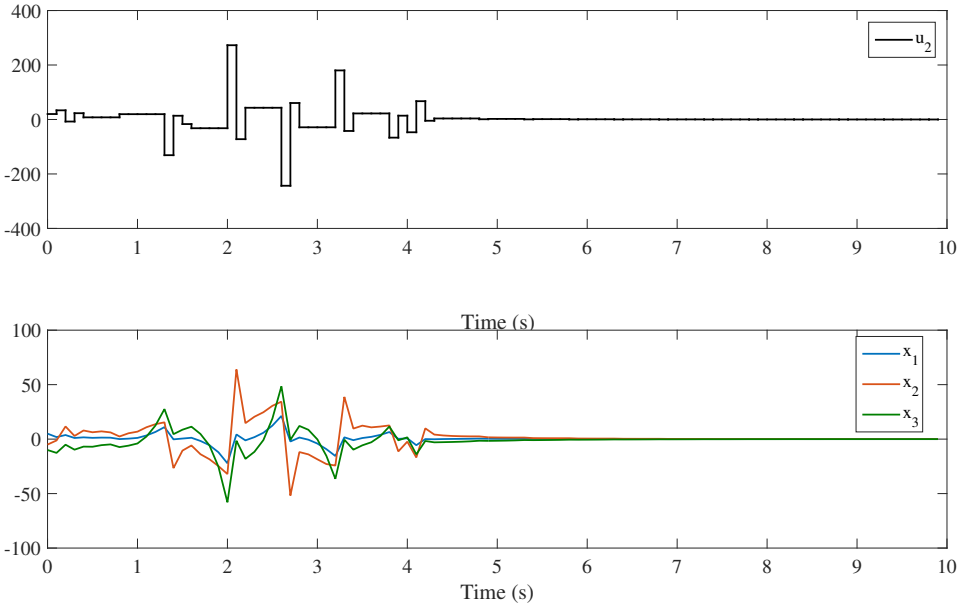

Figure 9. Control input and states of the HSA model by using the event-triggered ADP-based controller.

To illustrate the benefits of the event-triggered ADP method, the control input and the states of the original HSA system described by (2.10) and (2.11), as obtained by using the event-triggered ADP-based controller is shown in Figure 9.

The comparison of sampling numbers by using the event-triggered ADP controller versus the ADP controller with periodic sampling is shown in Figure 10.

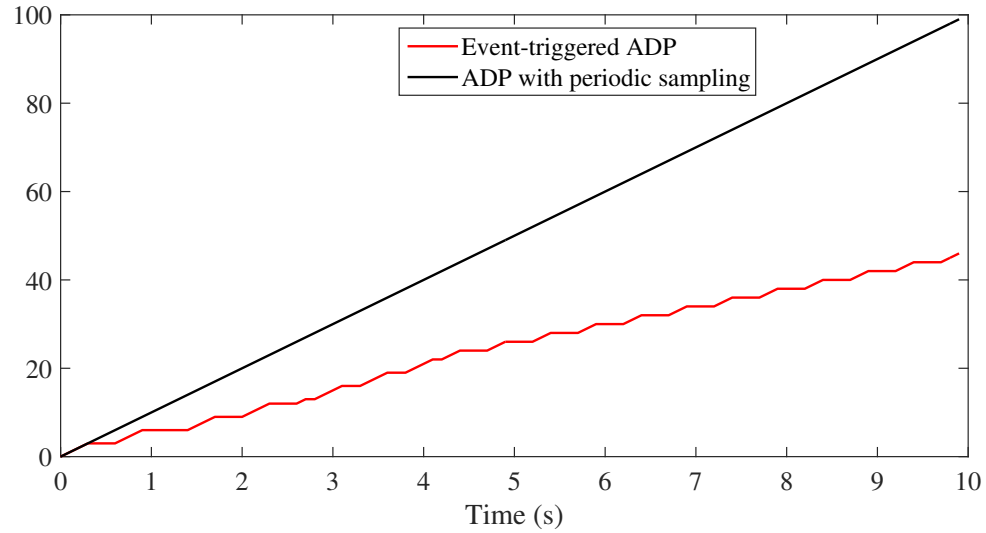

Figure 10. Comparison of the total sampling numbers.

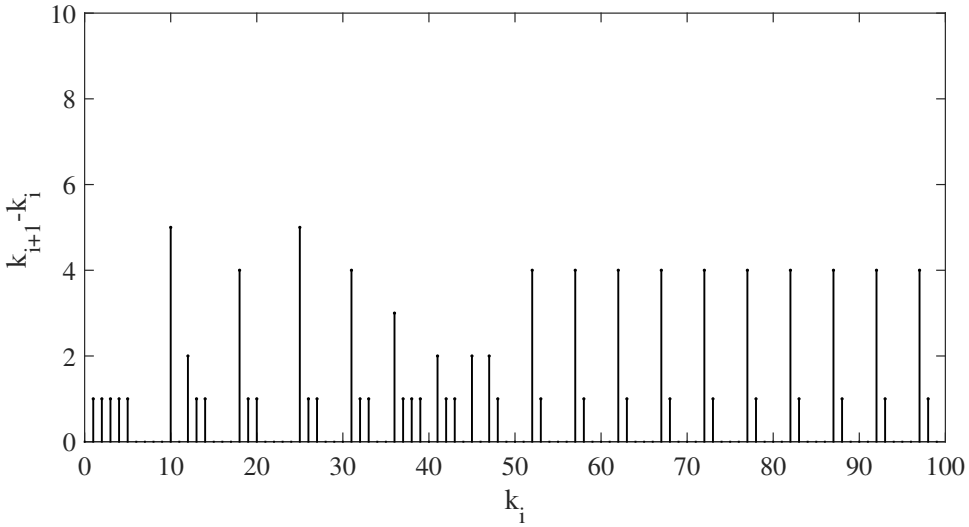

Figure 11. Sequence of steps of event-triggered sampling.

It can be observed that similar control effects have been achieved by the two methods, however, for the event-triggered ADP method, the control input is updated only when the squared norm of the triggering error reaches the threshold, and it is kept constant otherwise. It is also shown that about

54% communication between the controller and the HSA is reduced by using the event-triggered ADP method instead of the ADP method. The sequence of steps of event-triggered sampling is depicted in Figure 11.

5. Conclusions

This paper has considered the event-triggered data-driven optimal controller of the HSA with completely unknown dynamics as based on an ADP framework. A basic advantage of the presented control methodology is its ability to avoid the knowledge of entire system dynamics, which is very important in real conditions. By using the output feedback and the state reconstruction method an applied ADP-based control technique has been shown to be a useful tool for digital implementation in a real HSA. For that purpose, a discrete-time control policy was iteratively learned based on the discretized HSA model. The learned control policy very efficiently ensures online solutions to data-driven optimal control problems for the HSA. The presented online control policy only uses measured input/output data to learn the optimal control gain. Then, to reduce the communication between the controller and the HSA, an output feedback event-triggered ADP controller has been designed. The simulation results have shown the validity and effectiveness of the applied control approach for the HSA.

Acknowledgments

This research was supported in part by the Serbian Ministry of Education, Science and Technological Development under grant 451-03-47/2023-01/200108, the National Natural Science Foundation of China under grants 61773181, 61976081, 62073001, 62103293 and 62203153, 111 Project under grant B23008, the Fundamental Research Funds for the Central Universities under grant JUSRP51733B, the Anhui Provincial Key Research and Development Project under grant 2022i01020013 and the Natural Science Fund for Excellent Young Scholars of Henan Province under grant 202300410127.

Conflict of interest

The authors declare that there is no conflict of interest.

References

1. J. Vyas, B. Gopalsamy, H. Joshi, *Electro-Hydraulic Actuation Systems: Design, Testing, Identification and Validation*, 1st edition, Springer, Singapore, 2019. https://doi.org/10.1007/978-981-13-2547-2
2. A. Vacca, G. Franzoni, *Hydraulic Fluid Power: Fundamentals, Applications, and Circuit Design*, 1st edition, John Wiley & Sons, Hoboken, New Jersey, 2021.
3. N. Manring, *Fluid Power Pumps and Motors: Analysis, Design, and Control*, 1st edition, McGraw-Hill Education, New York, 2013.
4. N. Nedic, V. Stojanovic, V. Djordjevic, Optimal control of hydraulically driven parallel robot platform based on firefly algorithm, *Nonlinear Dyn.*, **82** (2015), 1457–1473. https://doi.org/10.1007/s11071-015-2252-5

5. V. Stojanovic, N. Nedic, D. Prsic, Lj. Dubonjic, V. Djordjevic, Application of cuckoo search algorithm to constrained control problem of a parallel robot platform, *Int. J. Adv. Manuf. Technol.*, **87** (2016), 2497–2507. https://doi.org/10.1007/s00170-016-8627-z
6. V. Filipovic, N. Nedic, V. Stojanovic, Robust identification of pneumatic servo actuators in the real situations, *Forsch. Ingenieurwes.*, **75** (2011), 183–196. https://doi.org/10.1007/s10010-011-0144-5
7. J. F. Blackburn, G. Reethof, J. L. Shearer, *Fluid Power Control*, MIT Press, Cambridge, Massachusetts, 1960.
8. M. Jelali, A. Kroll, *Hydraulic Servo-Systems: Modelling, Identification and Control*, 1st edition, Springer, London, 2003. https://doi.org/10.1007/978-1-4471-0099-7
9. F. L. Lewis, D. Liu, *Reinforcement Learning and Approximate Dynamic Programming for Feedback Control*, 1st edition, John Wiley & Sons, Hoboken, New Jersey, 2013.
10. D. Bertsekas, *Reinforcement Learning and Optimal Control*, 1st edition, Athena Scientific, Belmont, Massachusetts, 2019.
11. D. Bertsekas, *Dynamic Programming and Optimal Control: Volume I*, 4th edition, Athena Scientific, Belmont, Massachusetts, 2012.
12. F. L. Lewis, D. Vrabie, V. L. Syrmos, *Optimal Control*, 3rd edition, John Wiley & Sons, Hoboken, New Jersey, 2012.
13. M. Tomás-Rodríguez, S. P. Banks, *Linear, Time-Varying Approximations to Nonlinear Dynamical Systems: With Applications in Control and Optimization*, 1st edition, Springer, London, 2010. https://doi.org/10.1007/978-1-84996-101-1
14. V. Stojanovic, D. Prsic, Robust identification for fault detection in the presence of non-Gaussian noises: application to hydraulic servo drives, *Nonlinear Dyn.*, **100** (2020), 2299–2313. https://doi.org/10.1007/s11071-020-05616-4
15. M. Mynuddin, W. Gao, Distributed predictive cruise control based on reinforcement learning and validation on microscopic traffic simulation, *IET Intel. Transport Syst.*, **14** (2020), 270–277. https://doi.org/10.1049/iet-its.2019.0404
16. M. Mynuddin, W. Gao, Z. P. Jiang, Reinforcement learning for multi-agent systems with an application to distributed predictive cruise control, in *American Control Conference (ACC)*, (2020), 315–320. https://doi.org/10.23919/ACC45564.2020.9147968
17. M. Davari, W. Gao, Z.P. Jiang, F. L. Lewis, An optimal primary frequency control based on adaptive dynamic programming for islanded modernized microgrids, *IEEE Trans. Autom. Sci. Eng.*, **18** (2020), 1109–1121. https://doi.org/10.1109/TASE.2020.2996160
18. A. van de Walle, F. Naets, W. Desmet, Virtual microphone sensing through vibro-acoustic modelling and Kalman filtering, *Mech. Syst. Signal Process.*, **104** (2018), 120–133. https://doi.org/10.1016/j.ymssp.2017.08.032
19. K. Maes, A. Iliopoulos, W. Weijtjens, C. Devriendt, G. Lombaert, Dynamic strain estimation for fatigue assessment of an offshore monopile wind turbine using filtering and modal expansion algorithms, *Mech. Syst. Signal Process.*, **76** (2016), 592–611. https://doi.org/10.1016/j.ymssp.2016.01.004

20. Y. H. Chang, Q. Hu, C. J. Tomlin, Secure estimation based Kalman filter for cyber-physical systems against sensor attacks, *Automatica*, **95** (2018), 399–412. https://doi.org/10.1016/j.automatica.2018.06.010
21. A. Cavallo, G. De Maria, C. Natale, S. Pirozzi, Slipping detection and avoidance based on Kalman filter, *Mechatronics*, **24** (2014), 489–499. https://doi.org/10.1016/j.mechatronics.2014.05.006
22. W. Gao, M. Huang, Z.P. Jiang, T. Chai, Sampled-data-based adaptive optimal output-feedback control of a 2-degree-of-freedom helicopter, *IET Control Theory Appl.*, **10** (2016), 1440–1447. https://doi.org/10.1049/iet-cta.2015.0977
23. J. J. Murray, C. J. Cox, G. G. Lendaris, R. Saeks, Adaptive dynamic programming, *IEEE Trans. Syst. Man Cybern. Part C Appl. Rev.*, **32** (2002), 140–153. https://doi.org/10.1109/TSMCC.2002.801727
24. P. J. Werbos, *Beyond Regression: New Tools for Prediction and Analysis in the Behavioral Sciences*, Ph.D thesis, Harvard University, 1974.
25. W. Gao, Z. P. Jiang, Learning-based adaptive optimal tracking control of strict-feedback nonlinear systems, *IEEE Trans. Neural Networks Learn. Syst.*, **29** (2017), 2614–2624. https://doi.org/10.1109/TNNLS.2017.2761718
26. T. Bian, Z.P. Jiang, Value iteration and adaptive dynamic programming for data-driven adaptive optimal control design, *Automatica*, **71** (2016), 348–360. https://doi.org/10.1016/j.automatica.2016.05.003
27. M. Roozegar, M. J. Mahjoob, M. Jahromi, Optimal motion planning and control of a nonholonomic spherical robot using dynamic programming approach: simulation and experimental results, *Mechatronics*, **39** (2016), 174–184. https://doi.org/10.1016/j.mechatronics.2016.05.002
28. J. L. Sun, C. S. Liu, An overview on the adaptive dynamic programming based missile guidance law, *Acta Autom. Sin.*, **43** (2017), 1101–1113.
29. Q. Hu, Robust adaptive sliding mode attitude maneuvering and vibration damping of three-axis-stabilized flexible spacecraft with actuator saturation limits, *Nonlinear Dyn.*, **55** (2009), 301–321. https://doi.org/10.1007/s11071-008-9363-1
30. W. Gao, Y. Jiang, Z. P. Jiang, T. Chai, Output-feedback adaptive optimal control of interconnected systems based on robust adaptive dynamic programming, *Automatica*, **72** (2016), 37–45. https://doi.org/10.1016/j.automatica.2016.05.008
31. K. J. Åström, Event based control, in *Analysis and Design of Nonlinear Control Systems* (eds. A. Astolfi, L. Marconi), Springer, Berlin, Heidelberg, (2007), 127–147. https://doi.org/10.1007/978-3-540-74358-3
32. W. P. M. H. Heemels, M. C. F. Donkers, A. R. Teel, Periodic event-triggered control for linear systems, *IEEE Trans. Autom. Control*, **58** (2012), 847–861. https://doi.org/10.1109/TAC.2012.2220443
33. B. Jiang, H. R. Karimi, Y. Kao, C. Gao, Takagi-Sugeno model based event-triggered fuzzy sliding-mode control of networked control systems with semi-Markovian switchings, *IEEE Trans. Fuzzy Syst.*, **28** (2019), 673–683. https://doi.org/10.1109/TFUZZ.2019.2914005

34. T. Liu, Z. P. Jiang, A small-gain approach to robust event-triggered control of nonlinear systems, *IEEE Trans. Autom. Control*, **60** (2015), 2072–2085. https://doi.org/10.1109/TAC.2015.2396645
35. Y. S. Ma, W. W Che, C. Deng, Z. G. Wu, Observer-based event-triggered containment control for MASs under DoS attacks, *IEEE Trans. Cybern.*, **52** (2021), 13156–13167. https://doi.org/10.1109/TCYB.2021.3104178
36. X. Wang, H. R. Karimi, M. Shen, D. Liu, L. W. Li, J. Shi, Neural network-based event-triggered data-driven control of disturbed nonlinear systems with quantized input, *Neural Networks*, **156** (2022), 152–159. https://doi.org/10.1016/j.neunet.2022.09.021
37. M. Shen, Y. Gu, J. H. Park, Y. Yi, W. W. Che, Composite control of linear systems with event-triggered inputs and outputs, *IEEE Trans. Circuits Syst. II Express Briefs*, **69** (2021), 1154–1158. https://doi.org/10.1109/TCSII.2021.3098820
38. X. Wang, M. Shen, J. H. Park, Event-triggered control of uncertain nonlinear discrete-time systems with extended state observer, preprint. https://doi.org/10.21203/rs.3.rs-644060/v1
39. A. Sahoo, H. Xu, S. Jagannathan, Neural network-based event-triggered state feedback control of nonlinear continuous-time systems, *IEEE Trans. Neural Networks Learn. Syst.*, **27** (2015), 497–509. https://doi.org/10.1109/TNNLS.2015.2416259
40. L. Ljung, *System Identification: Theory for the User*, 2^{nd} edition, Prentice-Hall, Upper Saddle River, New Jersey, 1999.
41. R. Pintelon, J. Schoukens, *System Identification: A Frequency Domain Approach*, 1^{st} edition, John Wiley & Sons, Hoboken, New Jersey, 2012.
42. C. R. Rojas, J. C. Aguero, J. S. Welsh, G. C. Goodwin, A. Feuer, Robustness in experiment design, *IEEE Trans. Autom. Control*, **57** (2011), 860–874. https://doi.org/10.1109/TAC.2011.2166294
43. A. Al-Tamimi, F. L. Lewis, M. Abu-Khalaf, Model-free Q-learning designs for linear discrete-time zero-sum games with application to H-infinity control, *Automatica*, **43** (2007), 473–481. https://doi.org/10.1016/j.automatica.2006.09.019
44. F. L. Lewis, K. G. Vamvoudakis, Reinforcement learning for partially observable dynamic processes: Adaptive dynamic programming using measured output data, *IEEE Trans. Syst. Man Cybern. Part B Cybern.*, **41** (2010), 14–25. https://doi.org/10.1109/TSMCB.2010.2043839
45. T. Chen, B. A. Francis, *Optimal Sampled-Data Control Systems*, 1^{st} edition, Springer, London, 1995. https://doi.org/10.1007/978-1-4471-3037-6
46. G. Hewer, An iterative technique for the computation of the steady state gains for the discrete optimal regulator, *IEEE Trans. Autom. Control*, **16** (1971), 382–384. https://doi.org/10.1109/TAC.1971.1099755
47. W. Gao, Y. Jiang, Z. P. Jiang, T. Chai, Adaptive and optimal output feedback control of linear systems: An adaptive dynamic programming approach, in *Proceeding of the 11th World Congress on Intelligent Control and Automation*, (2014), 2085–2090. https://doi.org/10.1109/WCICA.2014.7053043
48. W. Aangenent, D. Kostic, B. de Jager, R. van de Molengraft, M. Steinbuch, Data-based optimal control, in *Proceedings of the 2005, American Control Conference*, (2005), 1460–1465. https://doi.org/10.1109/ACC.2005.1470171

49. K. J. Åström, B. Wittenmark, *Adaptive Control*, 2^{nd} edition, Dover Publication Inc, Mineola, New York, 2008.

50. P. A. Ioannou, J. Sun, *Robust Adaptive Control*, 2^{nd} edition, Dover Publication Inc, Mineola, New York, 2012.

51. K. G. Vamvoudakis, F. L. Lewis, Multi-player non-zero-sum games: Online adaptive learning solution of coupled Hamilton–Jacobi equations, *Automatica*, **47** (2011), 1556–1569. https://doi.org/10.1016/j.automatica.2011.03.005

52. H. Xu, S. Jagannathan, F. L. Lewis, Stochastic optimal control of unknown linear networked control system in the presence of random delays and packet losses, *Automatica*, **48** (2012), 1017–1030. https://doi.org/10.1016/j.automatica.2012.03.007

AIMS Press